JOURNAL OF BACTERIOLOGY, Oct. 2010, p. 4944–4953 Vol. 192, No. 19
0021-9193/10/$12.00 doi:10.1128/JB.00294-10

Pyruvate Is Synthesized by Two Pathways in Pea Bacteroids with Different Efficiencies for Nitrogen Fixation▽

Geraldine Mulley,[1] Miguel Lopez-Gomez,[1] Ye Zhang,[2] Jason Terpolilli,[1] Jurgen Prell,[1] Turlough Finan,[2] and Philip Poole[1]*

Department of Molecular Microbiology, John Innes Centre, Norwich Research Park, Colney, Norwich NR4 7UH, United Kingdom,[1] and Department of Biology, McMaster University, 1280 Main St. W., Hamilton, Ontario, Canada L8S4K1[2]

Received 16 March 2010/Accepted 22 July 2010

Nitrogen fixation in legume bacteroids is energized by the metabolism of dicarboxylic acids, which requires their oxidation to both oxaloacetate and pyruvate. In alfalfa bacteroids, production of pyruvate requires NAD^+ malic enzyme (Dme) but not $NADP^+$ malic enzyme (Tme). However, we show that *Rhizobium leguminosarum* has two pathways for pyruvate formation from dicarboxylates catalyzed by Dme and by the combined activities of phosphoenolpyruvate (PEP) carboxykinase (PckA) and pyruvate kinase (PykA). Both pathways enable N_2 fixation, but the PckA/PykA pathway supports N_2 fixation at only 60% of that for Dme. Double mutants of *dme* and *pckA*/*pykA* did not fix N_2. Furthermore, *dme pykA* double mutants did not grow on dicarboxylates, showing that they are the only pathways for the production of pyruvate from dicarboxylates normally expressed. PckA is not expressed in alfalfa bacteroids, resulting in an obligate requirement for Dme for pyruvate formation and N_2 fixation. When PckA was expressed from a constitutive *nptII* promoter in alfalfa *dme* bacteroids, acetylene was reduced at 30% of the wild-type rate, although this level was insufficient to prevent nitrogen starvation. Dme has N-terminal, malic enzyme (Me), and C-terminal phosphotransacetylase (Pta) domains. Deleting the Pta domain increased the peak acetylene reduction rate in 4-week-old pea plants to 140 to 150% of the wild-type rate, and this was accompanied by increased nodule mass. Plants infected with Pta deletion mutants did not have increased dry weight, demonstrating that there is not a sustained change in nitrogen fixation throughout growth. This indicates a complex relationship between pyruvate synthesis in bacteroids, nitrogen fixation, and plant growth.

The largest input of available nitrogen in the biosphere comes from the biological reduction of atmospheric N_2 to ammonium (20). Most of this comes from legume-*Rhizobium* symbioses, which arise from infection of host plants and result in root nodules (21). Signaling between the plant and bacterium is initiated by plant-released flavonoids and related compounds, which elicit the synthesis of lipochitooligosaccharide Nod factors by rhizobia (21). Bacteria are trapped by curling root hairs that they enter via infection threads. These grow into a zone of newly induced meristematic cells in the cortex that form the origin of the nodule. Bacteria are released from infection threads by endocytosis and surrounded by a plant-derived symbiosome membrane. Plants provide differentiated bacteria (bacteroids) with dicarboxylic acids which energize N_2 reduction to ammonium for secretion back to the plant (24, 37). A simple exchange of dicarboxylates and ammonium is the classical model of nutrient exchange in nodules, but amino acid transport by pea bacteroids has also been shown to be essential (13). This is because bacteroids reduce the synthesis of branched-chain amino acids and become symbiotic auxotrophs that depend on their provision by the plant (25). Thus, when the two broad-specificity amino acid ABC transporters (Aap and Bra) of *Rhizobium leguminosarum* are mutated, N_2-fixing pea bacteroids are formed, but they have reduced chromosome numbers and persistence (25).

The transport of dicarboxylic acids occurs via the dicarboxylic transport system (Dct) and is essential for N_2 fixation in a wide variety of bacteroids (8, 28–29, 39). When nodule C_4-dicarboxylic acids have been measured, L-malate has proved the most abundant, suggesting that its oxidation is a key step in carbon flux in the bacteroid (30–31). Consistent with this, NAD^+ malic enzyme (*d*iphosphopyridine nucleotide-dependent *m*alic *e*nzyme; Dme) in *Sinorhizobium meliloti* is essential for N_2 fixation in alfalfa nodules, but $NADP^+$ malic enzyme (*t*riphosphopyridine nucleotide-dependent *m*alic *e*nzyme; Tme) is not (3, 5, 17–18). This indicates that L-malate imported into the bacteroid is either oxidized by malate dehydrogenase to oxaloacetate or oxidatively decarboxylated to pyruvate by Dme. Pyruvate is then converted to acetyl coenzyme A (acetyl-CoA) by pyruvate dehydrogenase, subsequently condensed with oxaloacetate to citrate by citrate synthase, and further metabolized by the tricarboxylic acid (TCA) cycle. In agreement with this, pea bacteroids have a strong transcriptional upregulation of the decarboxylating arm of the TCA cycle (citrate synthase, aconitase, and 2-ketoglutarate dehydrogenase), which agrees with the measured activities of these enzymes (11, 16). Furthermore, 2-ketoglutarate dehydrogenase mutants of *R. leguminosarum*, isocitrate dehydrogenase, and citrate synthase null mutants of *S. meliloti*, as well as citrate synthase mutants of *Sinorhizobium fredii*, are all Fix^- (12, 14, 19, 36). However, only 7% of citrate synthase activity is required in *S. meliloti* to obtain wild-type rates of nitrogen fixa-

* Corresponding author. Mailing address: Department of Molecular Microbiology, John Innes Centre, Norwich Research Park, Colney Lane, Norwich NR4 7UH, United Kingdom. Phone: (44) 1603 450750. Fax: (44) 1603 450758. E-mail: philip.poole@bbsrc.ac.uk.

▽ Published ahead of print on 30 July 2010.

tion (9). In *Bradyrhizobium japonicum*, 2-ketoglutarate dehydrogenase mutants have far fewer bacteroids, but these fix N_2 at rates similar to those of wild-type bacteria (22–24). Likewise, *B. japonicum* isocitrate dehydrogenase mutants and aconitase mutants that have lost 70% of enzyme activity fix N_2 at wild-type rates (34–35). Thus, while a complete TCA cycle is almost always important for full bacteroid development and proliferation, in mature bacteroids, either the decarboxylating arm is dispensable (soybean bacteroids) or its enzyme activity can be severely reduced (alfalfa bacteroids). Thus, we are faced with the paradox that while the decarboxylating arm of the TCA cycle in wild-type pea bacteroids is highly upregulated both for transcription and for enzyme activity, the activity of key enzymes such as citrate synthase can be substantially decreased in alfalfa bacteroids. Of course, measurements of transcription and enzyme activity are not the same as measurements of metabolic flux, so it is possible to substantially lower an enzyme's activity without altering the rate of a reaction. It is clear that there is insufficient information about metabolic flux in bacteroids to assess different pathways.

In this study, we mutated the *dme* gene in *R. leguminosarum* bv. *viciae* Rlv3841 in the expectation that it would be unable to fix N_2 on peas, but surprisingly, it proved fully effective. Therefore, we investigated the pathways of malate conversion to pyruvate in Rlv3841 and demonstrated that there are two pathways, Dme and phosphoenolpyruvate (PEP) carboxykinase (PckA)/pyruvate kinase (PykA).

MATERIALS AND METHODS

Bacterial strains and culture conditions. The bacterial strains, plasmids, and primers used in this study are detailed in Table 1. *Rhizobium* strains were grown at 28°C in either tryptone yeast extract (TY) (2) or acid minimal salts medium (AMS) (22) with 10 mM D-glucose, 10 mM di-sodium succinate, or 20 mM pyruvate as carbon sources and 10 mM NH_4Cl as the nitrogen source. Antibiotics were used at the following concentrations ($\mu g\ ml^{-1}$): streptomycin (St), 500; kanamycin (Km), 20; neomycin (Nm), 80; tetracycline (Tc), 5; gentamicin (Gm), 20 and spectinomycin (Sp), 100.

Genetic modification of bacterial strains. All DNA cloning and analysis were performed as previously described (32). PCRs were conducted with 30-μl samples, using GoTaq Green Master Mix (Promega), 10 to 30 ng genomic DNA, and 0.3 μM concentrations of primers. The cycling conditions were 1 cycle of 95°C for 3 min; 30 cycles of 95°C for 45 s, 58°C for 45 s, and 72°C for 2 min; and a final extension step of 72°C for 5 min.

The *dme* gene (RL2671) was amplified by PCR (2,434 bp) using primers p952 and p953 that contain a SpeI and XhoI restriction site and cloned into pCR8/GW/TOPO (pRU1889). An Ω kanamycin resistance cassette from pHP45Ω-Km was integrated into the XmnI site within *dme* and the *dme*::Ω-Km SpeI/XhoI fragment cloned into the suicide vector pJQ200SK (pRU1909). Plasmid pRU1909 was conjugated into Rlv3841, and cells were plated on TY agar with gentamicin and then on AMS agar supplemented with 10% sucrose, 10 mM NH_4Cl, and kanamycin to select for gene replacement. Strain RU3941 was confirmed to contain the expected *dme*::Ω-Km mutation by PCR mapping using p1001 and pOT forward primers.

The *tme* gene (RL0407) was amplified by PCR using primers p1058 and p1059 that contain a SpeI and XhoI restriction site and cloned into pCR2.1-TOPO (pRU1957). A Ω spectinomycin cassette from pHP45Ω-Sp was integrated into the SmaI site within *tme*, and the *tme*::Ω-Sp SpeI/XhoI fragment was cloned into the suicide vector pJQ200SK (pRU1958). Plasmid pRU1958 was conjugated into Rlv3841 and RU3941, and cells were plated on TY agar with gentamicin and then on AMS agar supplemented with 10% sucrose, 10 mM NH_4Cl, and spectinomycin to select for gene replacement. Strains RU4008 and RU4009 were found to contain the correct *tme*::Ω-Sp mutation by PCR mapping using pOT forward with either p1119 or p1120 in separate reactions.

The kanamycin cassette was removed from plasmid pRU1909 by inverse PCR using primers p1256 and p1257. The 7.5-kb PCR product was digested using NcoI and ligated to form plasmid pRU2071. This deleted 220 bp of the native *dme* and added an NcoI site. The final protein has a native translation of bp 1 to 1295 of *dme* but has a C terminus resulting from frame-shifted translation of 160 bp. Plasmid pRU2071 was conjugated into RU3941 and RU4009, and cells were plated on TY agar with gentamicin and then on AMS agar supplemented with 10% sucrose and 10 mM NH_4Cl and subsequently counterselected on kanamycin to confirm loss of the kanamycin cassette. The Δ_{220}*dme* deletion mutation was confirmed for strains RU4166 and RU4167 by PCR mapping using primers p1001 and p1281.

Precisely defined Δ*dme*, Δ*pta*, and Δ*me* deletion mutants were also isolated in Rlv3841. To do this, a complete *dme* gene (4,770 bp) was amplified using primers p1772/p1773, and the product was cloned into pCR2.1-TOPO, forming pRU2253. Deletions in pRU2253 were made by inverse PCR using primers p1774/p1775 (Δ*dme*; 2,364-bp deletion, forming pLMB96), p1774/p1776 (Δ*pta*; 990-bp deletion, forming pLMB97), and p1777b/p1778b (Δ*me*; 1,209-bp deletion, forming pLMB98). Primers p1777b and p1778b contain MfeI restriction sites allowing sticky-end religation of the vector, ensuring an in-frame fusion of the N terminus to the Pta domain. The PCR products of p1774/p1775 and p1774/p1776 were blunt-end ligated. In addition, p1776 contains two stop codons to ensure that a fusion protein was not generated by deletion of the C-terminal Pta domain of Dme. All religated vectors were confirmed to be correct by sequencing. Finally, the SpeI/DraI fragments of each deletion plasmid were cloned into pJQ200SK, forming pLMB99 (Δ*dme*), pLMB100 (Δ*pta*), and pLMB101 (Δ*me*). These plasmids were conjugated into RU3941, plated on TY agar with gentamicin and then on AMS agar with 10% sucrose and 10 mM NH_4Cl. They were counterselected on kanamycin to confirm loss of the kanamycin cassette, generating strains LMB139 (Δ*dme*), LMB141 (Δ*pta*), and LMB194 (Δ*me*). The deletion mutations were confirmed by PCR mapping using primers pr159 and pr160. For complementation studies, the entire *dme* gene, the *me* domain, and the *pta* domain were cloned as NcoI/HindIII fragments from pRU2253, pLMB97, and pLMB98 into the stable broad-host-range plasmid pJP2, forming pLMB127, pLMB129, and pLMB128, respectively.

A 589-bp fragment from *pykA* (RL4060) was PCR amplified using primers p1371 and p1372 and cloned into HindIII-digested pK19mob using an In-Fusion Dry-Down PCR cloning kit (Clontech) to form plasmid pRU2099. Plasmid pRU2009 was conjugated into Rlv3841, RU4008, RU4166, and RU4167, and cells were plated on TY with kanamycin to select for pK19 integrations within *pykA*. The *pykA*::pK19 mutations were confirmed by PCR mapping for strains RU4291, RU4292, RU4293, and RU4294 by using primers p1373 and pK19A.

A 562-bp fragment from *pckA* (RL0037) was PCR amplified using primers BD_pckA_for and BD_pckA_rev and cloned into HindIII-linearized pK19mob using an In-Fusion Dry-Down PCR cloning kit (Clontech) to form plasmid pRU2047. Plasmid pRU2047 was conjugated into Rlv3841, RU4008, RU4166, and RU4167, and cells were plated on TY with kanamycin to select for pK19 integrations within *pckA*. The *pckA*::pK19 mutations were confirmed for strains RU4039, RU4334, RU4335, and RU4336 by PCR mapping using primers p1370 and pK19A.

A functional *pckA* gene, including the native ribosome binding site, was amplified from 3841 genomic DNA using the high-fidelity Phusion enzyme (Finnzymes) at 66°C for annealing and using primers pr51 and pr52. The PCR product was restriction digested with BamHI/XbaI (sites incorporated into p51/p52) and cloned into the BglII/XbaI restriction sites of the stable expression vector pJP2neo (25) under the control of the constitutive *nptII* promoter, forming pLMB31.

qRT-PCR analysis. Cultures of strain Rlv3841 were grown in AMS with glucose and NH_4Cl and harvested in log phase (optical density at 600 nm [OD_{600}], ~0.3). To isolate RNA, cells were resuspended in RNAprotect (RNA stabilization reagent) as described by the manufacturer (Qiagen), and contaminating DNA was removed with Turbo DNase (Ambion). The RNA was quantified using an Experion automated electrophoresis station (Bio-Rad). RNA (250 ng) was amplified with a SenseAmp RNA amplification kit (Genisphere). The resulting RNA was again quantified and diluted to a concentration of 80 ng/μl. Primers were designed using VectorNTI 9 (Invitrogen) to yield amplicon sizes of ~200 bp. The primers pr189/pr190, pr191/pr192, and pr193/pr194 (Table 1) were used for quantitative real-time PCR (qRT-PCR) analysis of N-terminal, malic enzyme, and Pta domains, respectively. Malate dehydrogenase was used as a reference gene (p1310/p1311). The qRT-PCRs were performed in triplicate using a QuantiTect SYBR green RT-PCR kit (Qiagen, Germany) in reactions (20 μl) which contained primers at 0.5 μM and 80 ng of RNA. Controls lacking reverse transcriptase were included for each RNA sample. The PCR program was as follows: 30 min at 50°C; 15 min at 95°C; and 35 cycles of 15 s at 95°C, 30 s at 60°C, and 30 s at 72°C. The induction of each gene was calculated as 2 to the power of the ΔC_T (difference between cycle threshold values at the two

TABLE 1. Strains, plasmids, and primers

Strain, plasmid, or primer	Genotype or sequence[a]	Reference or source
Strains		
Rlv3841	St^r derivative of *R. leguminosarum* bv. *viciae* strain 300	10
RU3941	Rlv3841 *dme*::Ω, Km^r	This work
RU4008	Rlv3841 *tme*::Ω, Sp^r	This work
RU4009	Rlv3841 *dme*::Ω, Km^r; *tme*::Ω, Sp^r	This work
RU4166	Rlv3841 Δ_{220}*dme*	This work
RU4167	Rlv3841 $_{220}$*dme tme*::Ω, Sp^r	This work
RU4291	Rlv3841 *pykA*::pk19	This work
RU4292	Rlv3841 *pykA*::pk19 *tme*::Ω, Sp^r	This work
RU4293	Rlv3841 *pykA*::pk19 Δ_{220}*dme*	This work
RU4294	Rlv3841 *pykA*::pk19 Δ_{220}*dme tme*::Ω, Sp^r	This work
RU4039	Rlv3841 *pckA*::pk19	This work
RU4334	Rlv3841 *pckA*::pk19 *tme*::Ω, Sp^r	This work
RU4335	Rlv3841 *pckA*::pk19 Δ_{220}*dme*	This work
RU4336	Rlv3841 *pckA*::pk19 Δ_{220}*dme tme*::Ω, Sp^r	This work
LMB139	Rlv3841 Δ*dme*	This work
LMB141	Rlv3841 Δ*pta*	This work
LMB194	Rlv3841 Δ*me*	This work
RmP110	Wild-type *S. meliloti*	3
G455	*dme*::Tn*5* mutant of RmP110	3
G456	*dme*::Tn*5* mutant of RmP110	3
RmP1933	RmG455 containing pLMB31; St^r, Nm^r, Tc^r	This work
RmP1981	RmG456 containing pLMB31; St^r, Nm^r, Tc^r	This work
Plasmids		
pCR2.1-TOPO	T-overhang PCR product TOPO cloning vector, Km^r	Invitrogen
pCR8/GW/TOPO	Blunt PCR product TOPO cloning vector, Sp^r	Invitrogen
pHP45Ω-Sp	Plasmid containing Ω Sp cassette, Sp^r	26
pHP45Ω-Km	Plasmid containing Ω Km cassette, Km^r	6
pJP2	Broad host range plasmid, *gusA*, Tc^r	23
pJP2neo	pJP2 containing a constitutive NptII promoter	25
pJQ200SK	pACYC derivative, P15A origin of replication, Gm^r	27
pK19mob	pK19mob pUC19 derivative, *lacZ mob*, Nm^r	33
pLMB31	*pckA* cloned in pJP2neo	This work
pLMB96	Δ*dme* cloned in pCR2.1-TOPO	This work
pLMB97	*dme* Δ*pta* cloned in pCR2.1-TOPO	This work
pLMB98	*dme* Δ*me* cloned in pCR2.1-TOPO	This work
pLMB99	Δ*dme* cloned in pJQ200SK	This work
pLMB100	*dme* Δ*pta* cloned in pJQ200SK	This work
pLMB101	*dme* Δ*me* cloned in pJQ200SK	This work
pLMB127	*dme* cloned in pJP2	This work
pLMB128	*pta* cloned in pJP2	This work
pLMB129	*me* cloned in pJP2	This work
pRU1889	*dme* in pCR8/GW/TOPO	This work
pRU1909	*dme*::Ω, Km^r in pJQ200SK	This work
pRU1957	*tme* in pCR2.1-TOPO	This work
pRU1958	*tme*::Ω, Sp^r in pJQ200SK	This work
pRU2047	*pckA* in pK19	This work
pRU2071	Δ_{220}*dme* in pJQ200SK	This work
pRU2099	*pykA* in pK19	This work
pRU2253	*dme* cloned in pCR2.1	This work
Primers		
BD_pckA_for	TGATTACGCCAAGCTTCGCTGTTCATCCGCAATCT	
BD_pckA_rev	GCAGGCATGCAAGCTGTTTTCAGTCAGCGACCCGT	
pOTforward	CGGTTTACAAGCATAAAGC	
pK19A	ATCAGATCTTGATCCCCTGC	
p952	TTTACTAGTCTGGAGATCCAGGCGACCAAG	
p953	TTTCTCGAGTAAAGGGCGTCTGTCGTTAC	
p1001	GCAGGCACTTTTCTTCCACC	
p1058	TTTACTAGTTGCGCGAGCTGATGGACAT	
p1059	TTTCTCGAGGCGGTTTTCGGACGACATCAT	
p1119	TTCATCAACTGCGTGCGT	
p1120	GCAATGGCTAGAGCATGA	
p1256	TTTCCATGGTTGCAGGATTTCGAAGTCA	
p1257	TTTCCATGGAACTGGTCGAGATAGGCGTC	
p1281	TCTGGAAAGCGGTCGATCT	

Continued on following page

TABLE 1—*Continued*

Strain, plasmid, or primer	Genotype or sequence[a]	Reference or source
p1310	GCGATGACCTTCTCGGCATCA	
p1311	CATGGCGTCGAGCGGATTG	
p1370	ACCCGGCAATAGAGCTGGCA	
p1371	TGATTACGCCAAGCTATGACGGCATCAGCACCTTC	
p1372	GCAGGCATGCAAGCTACCGTCTGCTGATCGACGAC	
p1373	ATGGGTGACGACGCAATGC	
p1772	TTTACTAGTAGATTGAGCTCGACCGAA	
p1773	TTTACTAGTGAGGTGCAGCCATTGTTG	
p1774	TGACAAGTCGGCCAACGCCT	
p1775	ACATCAATCGGATACGGGCGA	
p1776	TCATCACTTCATGACGAAGCCTGA	
p1777b	TTTCAATTGTGCCTGCTCGTCGAAATC	
p1778b	TTTCAATTGGACGCCTATCTCGACCAG	
pr51	TTTTCTAGATTATTCTGCAGCGACTTTCA	
pr52	TTTGGATCCGGCAGCGAGCCTGAGCGAAG	
pr159	CCAAGGTGCCGGTATTTG	
pr160	GAATGGGAATGCCCGAAG	
pr189	CGCCAATCTCGTCGCTGTCA	
pr190	TTGAAGAGCACGGCCTTGCC	
pr191	TCTGGGTCCACGATCTCGAAGG	
pr192	TATTTTCGGCGAGCGTGCG	
pr193	TCGAAGGCCGTTACGAGAAGCA	
pr194	GCCACGCTGTGAAATCATCAGG	

[a] *pta*, phosphotransacetylase domain gene; *me*, malic enzyme domain.

conditions analyzed). Samples were calibrated against the absolute level of RNA.

Enzyme assays. Bacteria (100 ml) were grown overnight in AMS minimum medium supplemented with succinate (20 mM) and NH_4Cl (10 mM), harvested by centrifugation, washed twice with HEPES (50 mM; pH 7.5) containing dithiothreitol (DTT; 2 mM), resuspended in the same buffer (3 ml), ribolyzed for 30 s, and then centrifuged at 13,000 rpm and 4°C for 5 min. The supernatants were used as crude protein extract for enzyme assays. NAD^+ (Dme)- and $NADP^+$ (Tme)-dependent malic enzyme activities were determined for an assay mixture containing Tris/HCl (100 mM; pH 7.8), L-malate (30 mM), $MnCl_2$ (3 mM), KCl (50 mM), and NAD^+ or $NADP^+$ (0.25 mM) in a final volume of 0.5 ml. Reactions were initiated by the addition of protein extract (100 μl) and were incubated for 10 min at 30°C. Malic enzyme activity was determined by measuring pyruvate production as follows. To 0.5 ml of the assay sample, 2,4-dinitrophenylhydrazine (0.1%; 165 μl in 2 M HCl) was added, and the mixture was incubated for 10 min at room temperature. NaOH (835 μl of 2.5 M) was added, and the mixture was incubated for 10 min and centrifuged in a microcentrifuge for 5 min (13,000 rpm). The absorbance of the supernatant was read at 445 nm and compared to a standard curve value for pyruvate. Blank reaction mixtures contained the complete reaction after no incubation and/or reactions to which no extract had been added.

Plant experiments. *R. leguminosarum* bv. *viciae* strains were inoculated on surface-sterilized pea seeds (*Pisum sativum* cv. Avola) at sowing. Peas were grown in vermiculite (1-liter pots) in a controlled-environment room at 22°C with a day-night cycle of 8 h of light and 16 h of darkness for 3 to 4 weeks, fed N-free nutrient solution, and used for acetylene reduction at the time of flowering, as previously described (1). Acetylene reduction by peas was measured after growth in two separate controlled-environment rooms, at the University of Reading and the John Innes Centre, and data for the two sites are identified separately. Peas were grown (2-liter pots) for 6 weeks for dry weight determination.

Medicago sativa var. Iroquois was grown in Leonard assemblies and inoculated with various strains of *S. meliloti*. Triplicate pots of eight seedlings were grown, and plants were harvested 6 weeks after inoculation. Shoot dry weight and acetylene reduction were assayed as previously described (38).

RESULTS

Pyruvate is formed from dicarboxylates by two pathways. NAD^+ and $NADP^+$ malic enzyme (Dme and Tme, respectively) are best characterized with *S. meliloti*, for which it has been shown that the reaction catalyzed by Dme is essential for N_2 fixation (Fig. 1) (3–5). To investigate this with *R. leguminosarum*, an Ω interposon was introduced into the XmnI site of *dme*, producing strain RU3941 (Fig. 2). Sur-

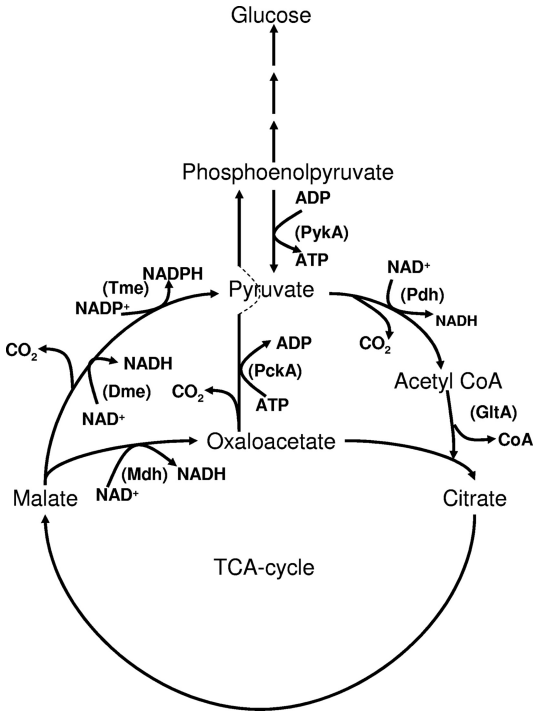

FIG. 1. Malate metabolism in *R. leguminosarum.* Dme, NAD^+ malic enzyme; GltA, citrate synthase; Mdh, malate dehydrogenase; PckA, phosphoenolpyruvate carboxykinase; Pdh, pyruvate dehydrogenase; PykA, pyruvate kinase; Tme, $NADP^+$ malic enzyme.

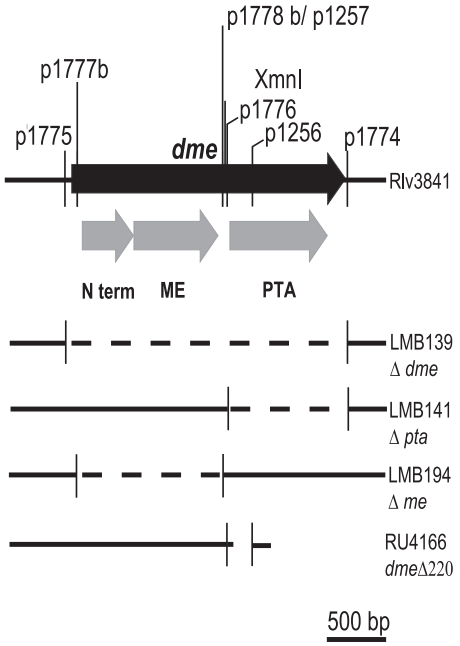

FIG. 2. Map of *dme* in *R. leguminosarum.* Deleted regions are shown with a dashed line. Primers numbers used for deletions are shown above the solid black arrow. N term, N terminus.

prisingly, RU3941 fixed nitrogen as did the double mutant RU4009 (*dme*Ω *tme*Ω) (Table 2). Notably, the total rates of N_2 fixation per plant, as measured by acetylene reduction, were significantly greater (140% to 150%) than that of the wild type for both strains. These data suggested that an alternative pathway exists for dicarboxylate metabolism in *R. leguminosarum* bacteroids that is not present or normally expressed in *S. meliloti.* To enable other possible pathways to be mutated, an unmarked deletion mutant (RU4166) was made with *dme* by deleting a 220-bp region (Δ_{220}*dme*) between the malic enzyme NAD^+ binding domain and the phosphotransacetylase domain (Fig. 2). This leaves 1 to 1,295 bp of the native *dme* with a frame-shifted 3′ end of 160 bp. Curiously, strain RU4166 reduced acetylene only at 58 to 73% of the wild-type rate, unlike the 140 to 150% measured for RU3941 and RU4009 (Table 2). When the Δ_{220}*dme* mutation was combined with a *tme* mutation (RU4167), acetylene was again reduced at 48% of the wild-type rate (Table 2). There is clearly a profound difference in the phenotype of *dme* mutants made with a C-terminal Ω insertion of an interposon relative to a C-terminal unmarked deletion. The reason for this is considered below, but first, we sought to discover the second *dme*-independent pathway for dicarboxylate metabolism.

Malate is the substrate for both malic enzyme and (via oxaloacetate) phosphoenolpyruvate carboxykinase (PckA), which is the first enzyme of gluconeogenesis (Fig. 1). Therefore, double *pckA* Δ_{220}*dme* (RU4335) and triple *pckA* Δ_{220}*dme tme*Ω (RU4336) mutants were isolated and shown to be unable to reduce acetylene, indicating a complete block in N_2 fixation (Table 2). Thus, the two pathways for conversion of malate to pyruvate in pea bacteroids are Dme and PckA. The product of the reaction catalyzed by PckA is phosphoenolpyruvate, which either can be used for gluconeogenesis or can be converted to pyruvate by pyruvate kinase (PykA) (Fig. 1). It can therefore be predicted that PykA should be essential for dicarboxylate catabolism in conjunction with PckA in a *dme* strain. Consistent with this, RU4294 (*pykA* Δ_{220}*dme tme*Ω) had only a trace

TABLE 2. Acetylene reduction of peas infected with various strains of *R. leguminosarum*[a]

Strain (genotype)	ARA	No. of harvests	Total no. of plants	Location	*P* value
Rlv3841 (wild type)	3.88 ± 0.18	5	40	RDG	
RU3941 (*dme*Ω)	5.78 ± 0.25	5	40	RDG	<0.001
RU4008 (*tme*Ω)	3.52 ± 0.17	2	10	RDG	0.395
RU4009 (*dme*Ω *tme*Ω)	5.56 ± 0.40	2	10	RDG	<0.001
RU4294 (*pykA* D_{220}*dme tme*Ω)	0.28 ± 0.17	1	5	RDG	<0.001
RU4336 (*pckA* D_{220}*dme tme*Ω)	0.01 ± 0.00	1	5	RDG	<0.001
RU4039 (*pckA*)	5.06 ± 0.69	2	15	RDG	0.061
RU4291 (*pykA*)	6.75 ± 0.61	1	5	RDG	<0.001
RU4166 (D_{220}*dme*)	2.24 ± 0.43	1	10	RDG	0.056
RU4335 (*pckA* D_{220}*dme*)	0.02 ± 0.01	1	5	RDG	<0.001
Rlv3841 (wild type)	2.61 ± 0.20	3	18	JIC	
RU3941 (*dme*Ω)	3.77 ± 0.52	2	11	JIC	0.005
RU4166 (D_{220}*dme*)	1.91 ± 0.12	1	4	JIC	0.010
RU4167 (D_{220}*dme tme*Ω)	1.24 ± 0.16	1	7	JIC	0.011
LMB139 (Δ*dme*)	1.65 ± 0.13	3	20	JIC	<0.001
LMB141 (Δ*pta*)	3.84 ± 0.27	2	14	JIC	<0.001
LMB194 (Δ*me*)	1.64 ± 0.20	1	8	JIC	0.029
RU4336/*pdme*	2.06 ± 0.14	1	7	JIC	0.962
RU4336/*ppta*	0	1	7	JIC	<0.001
RU4336/*pme*	2.14 ± 0.21	1	7	JIC	0.828

[a] Strains are shown with their genotype in parentheses. The number of independent plant harvests and total number of plants are shown for each strain. Harvests were conducted at two locations, the University of Reading (RDG) and the John Innes Centre (JIC). All samples were compared by one-way blocked analysis of variance (ANOVA) for plants infected with Rlv3841 from the same harvests. Strain RU3941, strain RU4166, and the wild type (3841) were harvested at both RDG and JIC. The *P* value from blocked ANOVA across both sites for RU3941 versus 3841 is <0.001, and that for RU4166 versus 3841 is 0.006. Rates of acetylene reduction (ARA) are in micromoles h^{-1} $plant^{-1}$ and are shown ± standard errors of the means (SEM). Plasmids pLMB127 (p*dme*), pLMB128 (p*pta*), and pLMB129 (p*me*) contain the whole *dme* gene, just the Pta domain, and just the malic enzyme domain, respectively.

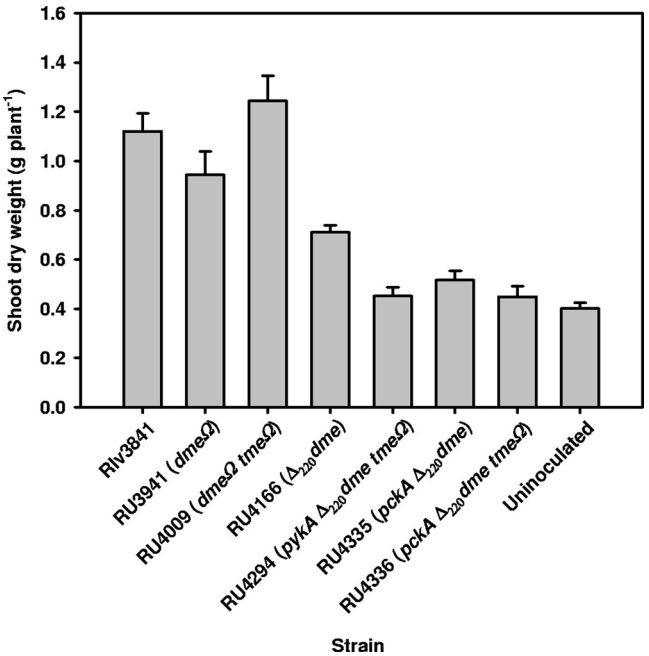

FIG. 3. Shoot dry weights of peas inoculated with various strains of *R. leguminosarum.* Dry weights were determined after 6 weeks of growth. Strains are shown with their genotype in parentheses. Twenty-eight plants were used for Rlv3841, 26 were used for RU3941, and 16 were uninoculated; for all other strains, 7 plants were used. All treatments were compared by *t* test, and results were significantly different from those for Rlv3841 ($P < 0.05$) except in the cases of RU3941 and RU4009. Values are means ± SEM.

of acetylene reduction (Table 2), indicating that it is blocked in both the Dme and PckA/PykA pathways.

In all cases, the Fix$^-$ strains produced yellow, stunted plants with numerous white nodules. Dry weights of 6-week-old pea plants inoculated with RU3941 (*dme*Ω) or RU4009 (*dme*Ω *tme*Ω) were not significantly different from those inoculated with Rlv3841 (Fig. 3). This result suggests that the elevated rate of acetylene reduction measured at the flowering point for RU3941 and RU4009 do not indicate a higher rate of N_2 fixation throughout growth, which should lead to greater plant growth. Acetylene reduction was measured at flowering (4 weeks), which is the peak rate of N_2 fixation in peas, so the data in Table 2 indicate only a change in the peak rate of N_2 fixation. Plants inoculated with bacteria with mutations of the *pckA* and *dme* (RU4335 and RU4336) or *pykA* and *dme* (RU4294) genes were indistinguishable from uninoculated controls, consistent with their being unable to fix N_2. Plants inoculated with RU4166 (Δ_{220}*dme*) showed an intermediate phenotype resulting in a dry weight significantly different ($P < 0.01$) from that of all other strains. This is consistent with its intermediate rate of N_2 fixation (60%) relative to that of the wild type.

Growth on dicarboxylates requires either the *dme* or the *pckA*/*pykA* pathway. *dme* and even *dme tme* mutants are still able to grow in laboratory culture on dicarboxylates such as succinate, almost certainly because they still possess the *pckA*/*pykA* pathway to make pyruvate from malate (Table 3). As expected, *pckA* mutant strains cannot grow on any organic acids, including pyruvate (monocarboxylate) or succinate (dicarboxylate), because they have lost the ability to make sugars via gluconeogenesis. A more useful test is to examine *pykA* mutants, because pyruvate kinase is not required for gluconeogenesis. The *pykA dme* double mutant (RU4293) failed to grow on dicarboxylates but retained the ability to grow on pyruvate (Table 3). This result confirms that Dme and PckA/PykA are the only pathways expressed in laboratory cultures of Rlv3841 for making pyruvate from dicarboxylates.

Effect of removing the phosphotransacetylase domain. As already described, there is a profound difference in the peak rates of acetylene reduction between *dme* mutants made with a C-terminal insertion of an Ω interposon relative to a C-terminal deletion (Table 2). To clarify this contradiction, three strains with precise deletions in the *dme* gene were made (Fig. 2). In the first strain (LMB139), the whole of the *dme* gene was deleted. In the second strain (LMB141), the phosphotransacetylase domain was deleted (Δ*pta*), forming a protein M1-K444 with the N-terminal and malic enzyme domain intact. A stop codon was inserted after K444. In the third strain (LMB194), the malic enzyme domain was removed (Δ*me*) by fusing A23 to D426 (a QL linker was inserted between these residues), leaving a complete Pta domain. These strains were inoculated onto peas, and acetylene reduction was measured at flowering (Table 2). The strain with a complete deletion of the *dme* gene (LMB139) reduced acetylene at 63% of the wild-type rate, as did a strain lacking the malic enzyme domain (LMB194). This result is almost identical to those for strains RU4166 (Δ_{220}*dme*) and RU4167 (Δ_{220}*dme tme*Ω). Thus, the complete loss of Dme reduced peak N_2 fixation to around 60% of that of the wild type. In the complete absence of Dme, only the PckA/PykA pathway is present, suggesting that it supports N_2 fixation at only 60% of the wild-type rate. It also implies that the Δ_{220}*dme* deletion results in a complete loss of any activity of the Dme protein. This is unsurprising, since a 220-bp deletion, which also causes the formation of a frame-shifted carboxy terminus, would probably result in misfolding of the

TABLE 3. Growth on different carbon sources[a]

Strain	Growth on AMS agar supplemented with NH_4Cl and:		
	Glucose	Succinate	Pyruvate
RL3841 (wild type)	+	+	+
RU3941 (*dme*::Ω)	+	+	+
RU4008 (*tme*::Ω)	+	+	+
RU4009 (*dme*::Ω; *tme*::Ω)	+	+	+
RU4166 (Δ_{220}*dme*)	+	+	+
RU4167 (Δ_{220}*dme tme*::Ω)	+	+	+
RU4291 (*pykA*::pk19)	+	+	+
RU4292 (*pykA*::pk19 *tme*::Ω)	+	+	+
RU4293 (*pykA*::pk19 Δ_{220}*dme*)	+	−	+
RU4294 (*pykA*::pk19 Δ_{220}*dme tme*::Ω)	+	−	+
RU4039 (*pckA*::pk19)	+	−	−
RU4334 (*pckA*::pk19 *tme*::Ω)	+	−	−
RU4335 (*pckA*::pk19 Δ_{220}*dme*)	+	−	−
RU4336 (*pckA*::pk19 Δ_{220}*dme tme*::Ω)	+	−	−

[a] Growth on AMS agar supplemented with 10 mM NH_4Cl and 10 mM glucose, 20 mM succinate, or 20 mM pyruvate as the sole carbon source after 5 days of growth at 28°C.

TABLE 4. Nodulation properties of various strains[a]

Strain (genotype)	No. of nodules	Nodule fresh wt (mg)
Rlv3841 (wild type)	115 ± 11.8	260 ± 30
RU3941 (*dme*::Ω)	134 ± 17.1	340 ± 29.4
LMB139 (Δ*dme*)	111 ± 15.5	197 ± 21.2
LMB141 (Δ*pta*)	123 ± 8.6	366 ± 20.0*

[a] Six plants were harvested for each inoculated strain. The number of nodules and total nodule fresh weight per plant for each strain were compared by *t* test to Rlv3841, and those that are significantly different ($P < 0.05$) are indicated with an asterisk. RU3941 has a *P* value of 0.067. Values ± SEM are shown.

TABLE 5. Malic enzyme activity[a]

Strain (genotype)	NAD^+-dependent ME activity	$NADP^+$-dependent ME activity
Rlv3841 (wild type)	87 ± 7.6 (12)	57.8 ± 6.3 (2)
RU3941 (*dme*::Ω, Km^r)	62 ± 10.5 (5)	48.0 ± 0.7 (2)
RU4008 (*tme*::Ω, Sp^r)	84.5 ± 6.4 (2)	23.9 ± 4.4 (2)
RU4009 (*dme*::Ω, Km^r; *tme*::Ω Sp^r)	27.5 ± 20.4 (2)	10.8 ± 1.0 (2)
RU4166 (Δ_{220}*dme*)	37.9 ± 9.5 (6)*	ND
RU4167 (Δ_{220}*dme tme*::Ω, Sp^r)	17.6 ± 2.2 (3)*	ND
LMB139 (Δ*dme*)	38.8 ± 3.8 (7)*	ND
LMB139/p*dme*	147.1 ± 29.7 (3)*	ND
LMB139/p*me*	34.2 ± 4.7 (3)*	ND
LMB139/p*pta*	28.8 ± 7.4 (3)*	ND
LMB141 (Δ*pta*)	45.3 ± 1.1 (3)*	ND
LMB194 (Δ*me*)	23.7 ± 4.5 (3)*	ND

[a] Activity measured in cell extracts from cultures grown in AMS with 20 mM succinate and 10 mM NH_4Cl. Rates are $nmol^{-1}$ mg of $protein^{-1}$ min^{-1} ± the SEM calculated from the number of independent biological replicates shown in parentheses. Activities for each strain were compared by *t* test to that of Rlv3841, and those that are significantly different ($P < 0.05$) are indicated with an asterisk. Strains with only two independent replicates were not compared by *t* test. ND, not determined.

whole protein. In dramatic contrast, LMB141 (Δ*pta*) reduced acetylene at 147% of the wild-type rate, which is almost identical to results for strains containing the *dme*Ω insertion. As stated above, the increased peak rate of acetylene reduction per plant measured at 4 weeks did not lead to a greater plant weight at 6 weeks. Thus, changes in the type of *dme* mutation somehow alter the peak capacity for N_2 fixation but do not alter overall plant growth and therefore almost certainly do not alter the total amount of N_2 fixed. There was no significant difference in the numbers of nodules measured at 4 weeks for any of the strains. However, there was a tendency for strains with the PTA domain deleted to have larger nodules with a greater total fresh weight (Table 4), although the probability value for LMB141 compared to that for Rlv3841 is only 0.067. Thus, most of the increased acetylene reduction at 4 weeks probably results from a plant response to the presence of Pta-deleted strains.

Since Ω interposons have transcriptional terminators at both ends, the insertion of Ω Km in the XmnI site of the *dme* gene in RU3941 should remove the Pta domain but leave the N-terminal and malic enzyme domains intact. This would explain why RU3941 behaves like LMB141 (Δ*pta*) with regard to acetylene reduction *in planta*. To investigate this, expression of mRNA for the N-terminal, malic enzyme, and Pta domains of the *dme* gene in Rlv3841 and RU3941 were compared by qRT-PCR. The N-terminal and NAD^+ binding domains of RU3941 had C_T values that were only 0.6 cycle lower and 0.6 cycle higher than that for Rlv3841, respectively. In contrast, the C_T value of the *pta* domain of RU3941 was 7 cycles higher than that for Rlv3841, indicating a 128-fold reduction in mRNA. Thus, strains containing the Ω insertion in the XmnI site of the *dme* gene have a *pta* deletion similar to that in LMB141 (Δ*pta*).

The malic enzyme domain has malic enzyme activity. Malic enzyme is notoriously difficult to accurately quantify in crude extract because of cross-activity between NAD^+ and $NADP^+$ malic enzymes. In addition, malate dehydrogenase oxidizes malate to oxaloacetate. Pyruvate and oxaloacetate react with hydrazine to produce similar hydrazones, which are then both measured as a product of the malic enzyme reaction. This is reflected in large errors in measured activities (Table 5). However, in spite of these difficulties, mutation of either NAD^+ or $NADP^+$ malic enzyme lowered the total measured activity. Furthermore, the lowest measured activity was obtained for the double *dme tme* mutant RU4167. The complete deletion of the *dme* (LMB139), *pta* (LMB141), or *me* (LMB194) domain also reduced the detectable NAD^+ malic enzyme activity. It has already been demonstrated that *S. meliloti* Dme lacking the Pta domain expressed in *Escherichia coli* EJ1321 retains only 10% of malic enzyme activity (18). This residual activity was not detectable in our assays of malic enzyme, which is hardly surprising for such a noisy assay conducted using crude extracts.

Overexpression in LMB139 (Δ*dme*) of the full-length Dme, but not the Me or Pta domains, increased the detectable malic enzyme activity above the wild-type rate (Table 5). The failure to detect an increase in malic enzyme activity when the Me domain was overexpressed may be due to it retaining only a low level of activity that would be difficult to detect in crude extracts. To investigate the effects of these domains on N_2 fixation, the same plasmids were introduced into the Fix^- strain RU4336 (*pckA* Δ_{220}*dme tme*Ω). N_2 fixation was restored to the wild-type rate in RU4336 by both the full-length Dme and the Me domain. This indicates that the Me domain retains sufficient malic enzyme activity to fully restore N_2 fixation in spite of our inability to measure it. In this regard, it is different from the situation with *S. meliloti*, in which reducing Dme activity also reduced N_2 fixation (17).

Mutation of PckA or PykA activity increases acetylene reduction at flowering. Mutation of *pckA* (RU4039) also increased the rate of acetylene reduction at flowering to 140% of the wild-type rate, although the probability value is only 0.061 (Table 2). However, mutation of *pykA* (RU4291) also increased the rate of acetylene reduction at flowering to 174% of the wild-type rate ($P < 0.001$). Thus, blocking the PckA/PykA pathway or reducing the Dme pathway by deletion of Pta increases peak acetylene reduction at flowering.

Expression of PckA in *S. meliloti* bacteroids enables weak N_2 fixation. Dme activity is essential for N_2 fixation in alfalfa nodules infected by *S. meliloti* (3, 5, 17–18). Since *S. meliloti* bacteroids do not express PckA activity, we considered the possibility that this might result in their obligate requirement for Dme activity (7). To test this, *pckA* from *R. leguminosarum* was cloned under the control of a constitutive neomycin phosphotransferase promoter in the environmentally stable vector pJP2. This clone was then conjugated into two *S. meliloti*

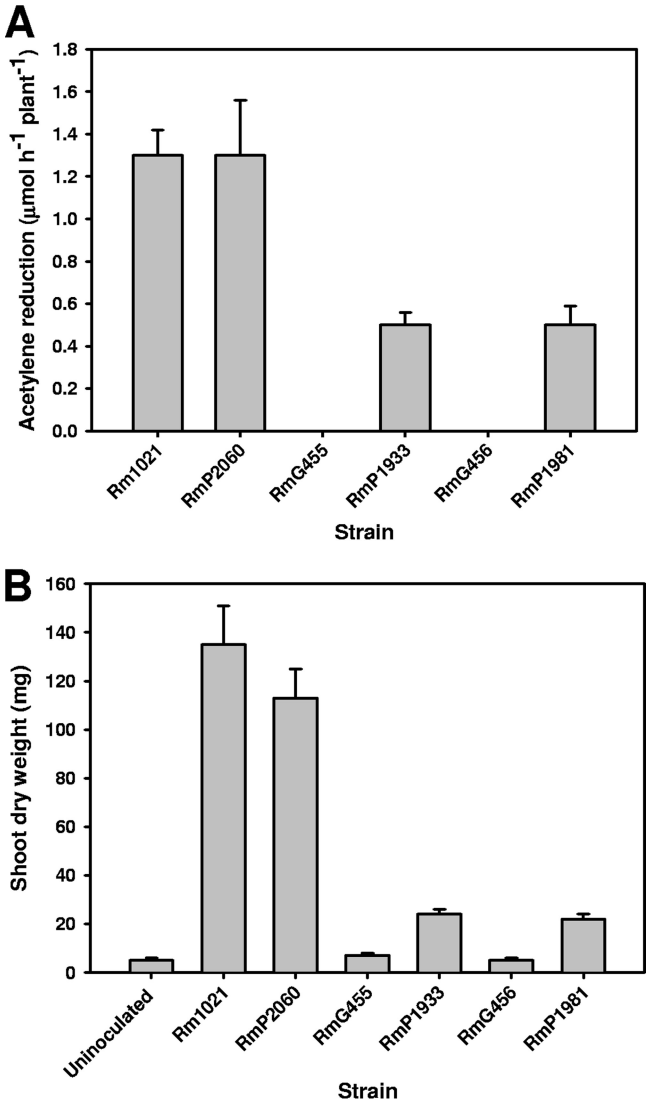

FIG. 4. PckA expression partially restores symbiotic N_2 fixation to *S. meliloti dme* mutants. (A) Nitrogenase activity (acetylene reduction in μmol h^{-1} $plant^{-1}$). (B) Shoot dry weights per plant. Plants were harvested 6 weeks after inoculation. Panels A and B represent two independent experiments with triplicate pots per strain and eight plants per pot; values are means ± SEM for triplicate samples.

strains mutated in *dme* (G455 and G456), forming P1933 and P1981, respectively. The parent strains (G455 and G456) are Fix^- (3), but a low level of acetylene (30%) was reduced by P1933 and P1981 (Fig. 4A). There was also a small increase in dry weight of P1933 and P1981 relative to that of uninoculated plants (Fig. 4B). Thus, the PckA pathway can contribute to pyruvate formation in alfalfa bacteroids but only at a very low level that is insufficient to prevent severe nitrogen starvation in the host.

DISCUSSION

It is well established that Dme is essential for N_2 fixation in alfalfa (3, 5, 17–18). It was therefore very surprising that *dme* mutants and even *dme tme* double mutants fixed N_2 in the pea. This suggested that an alternative to the Dme pathway for conversion of dicarboxylic acids to pyruvate exists in *R. leguminosarum* Rlv3841. Mutational analysis revealed that the second pathway for pyruvate synthesis occurs via phosphoenolpyruvate carboxykinase and pyruvate kinase. Double mutants in both pathways (*dme pykA*) were unable to grow on succinate, although they grew well on pyruvate. Thus, the blockage is in pyruvate synthesis and not gluconeogenesis.

Mutation of *dme* and *pckA*/*pykA* genes prevents N_2 fixation on peas, which is consistent with dicarboxylates being the energy source for bacteroids. However, the Dme pathway supports a higher rate of N_2 fixation than PckA/PykA, with *dme* deletion mutants reducing acetylene at only approximately 60% of wild-type rates and having significantly lower plant dry weights. In contrast, *pckA* mutants are either unaltered or actually show higher rates of acetylene reduction (Fig. 2). This suggests, as discussed below, that the Dme reaction is more favorable for N_2 fixation.

It is interesting to compare pea nodules to alfalfa nodules. Alfalfa infected with *S. meliloti* Sm1021 mutated in the *dme* gene alone is Fix^-. However, *S. meliloti* bacteroids do not express PckA, in contrast with *R. leguminosarum* bacteroids (7, 15). This suggested that a *dme* mutant of Sm1021 may be Fix^-, because it lacks the second pathway for pyruvate synthesis in bacteroids. However, expression of PckA restored only a low level of N_2 fixation in alfalfa, one that was insufficient to rescue plant growth. While we cannot rule out a trivial effect, such as insufficient pyruvate kinase, this result suggests that there may be other differences in, for example, energy charge or redox poise that force most dicarboxylate metabolism through Dme in Sm1021. However, it is most noteworthy that in both peas and alfalfa, the Dme pathway is preferred for N_2 fixation, and so the differences are only a matter of degree. It is also particularly interesting that Dme cannot be replaced by Tme in *S. meliloti* 1021, even when Tme is overexpressed from a Dme promoter (17). This suggests an obligate use of NAD^+ rather than $NADP^+$.

A second unexpected finding in this study was that the serendipitous removal of the Pta domain of Dme, which removes most but not all malic enzyme activity, increased the peak rate of N_2 fixation as measured by acetylene reduction to 140 to 150% of that of the wild type. This initially seemed very strange, because the malic enzyme pathway supports higher rates of nitrogen fixation and plant dry weights than the PckA/PykA pathway. Crucially, the increased rate of N_2 fixation was dependent on the retention of a trace of malic enzyme activity. If NAD^+ malic enzyme was completely deleted or inactivated (e.g., LMB194 or RU4166 Δ_{220}*dme*), then N_2 fixation was reduced to 60% of the wild-type rate. However, we inferred that in the absence of the Pta domain, malic enzyme retains a trace of activity, because it is able to complement N_2 fixation in a strain with complete deletions of both *dme* and *pckA* (RU4336 p*me*) (Fig. 3). We did attempt to measure the residual activity of malic enzyme when the Pta domain was deleted but were unable to do so because of the technical difficulty associated with its assay in crude extracts. However, it has already been shown that when *S. meliloti* Dme lacking the Pta domain was expressed in *E. coli*, only 10% of the activity of the full-length protein remained (18). Blocking the PckA/PykA

pathway by deletion of the *pckA* or *pykA* gene also increased the rate of nitrogen fixation at flowering in peas. Nitrogen fixation is at its highest at flowering in peas, and this is when acetylene reduction (around 4 weeks) was measured. The increase in the peak rate of acetylene reduction was accompanied by an increase in nodule fresh weight although not nodule number (Table 4). Increased nodule mass explains almost all the increased acetylene reduction, indicating that this is a plant response to an alteration in the microsymbiont. One possibility is that partially blocking pyruvate synthesis in developing bacteroids triggers a plant response that increases nodule mass. It could be in response to a failure of early bacteroids to make a signaling molecule or initially low rates of N_2 fixation, which may be caused by reduced pyruvate synthesis. The increased nodule mass in response to reduced early performance of the microsymbiont may result in a temporary overshoot in acetylene reduction at flowering. However, there is no change in the dry weight of peas harvested at 6 weeks, so this effect is not sustained. While the relationship between the Dme and PckA/PykA pathways is very complex, it is very clear how crucial the rate of pyruvate synthesis is to N_2 fixation. Partially blocking pyruvate synthesis (Pta deletion of Dme or mutation of PckA/PykA) may result in an overshoot in symbiotic performance at flowering, but completely deleting Dme dramatically lowers both peak acetylene reduction and plant dry weight. Evidently, the plant cannot compensate for a complete loss of Dme activity in bacteroids by increasing nodule mass (Table 4). This suggests either that Dme makes the greatest contribution to pyruvate synthesis or that its coupled production of NADH is important to N_2 fixation. Overall, these data show that the Dme and PckA/PykA pathways must interact with each other and are key steps in bacteroid carbon metabolism.

ACKNOWLEDGMENTS

This work was supported by a grant from the Biotechnology and Biological Sciences Research Council, United Kingdom (BB/F013159/1). Work in the laboratory of T.F. was supported by the Natural Sciences and Engineering Research Council of Canada.

REFERENCES

1. **Allaway, D., E. Lodwig, L. A. Crompton, M. Wood, T. R. Parsons, T. Wheeler, and P. S. Poole.** 2000. Identification of alanine dehydrogenase and its role in mixed secretion of ammonium and alanine by pea bacteroids. Mol. Microbiol. **36:**508–515.
2. **Beringer, J. E.** 1974. R factor transfer in *Rhizobium leguminosarum*. J. Gen. Microbiol. **84:**188–198.
3. **Driscoll, B. T., and T. M. Finan.** 1993. NAD^+-dependent malic enzyme of *Rhizobium meliloti* is required for symbiotic nitrogen fixation. Mol. Microbiol. **7:**865–873.
4. **Driscoll, B. T., and T. M. Finan.** 1996. $NADP^+$-dependent malic enzyme of *Rhizobium meliloti*. J. Bacteriol. **178:**2224–2231.
5. **Driscoll, B. T., and T. M. Finan.** 1997. Properties of NAD^+- and $NADP^+$-dependent malic enzymes of *Rhizobium* (*Sinorhizobium*) *meliloti* and differential expression of their genes in nitrogen-fixing bacteroids. Microbiology **143:**489–498.
6. **Fellay, R., J. Frey, and H. Krisch.** 1987. Interposon mutagenesis of soil and water bacteria: a family of DNA fragments designed for *in vitro* insertional mutagenesis of gram-negative bacteria. Gene **52:**147–154.
7. **Finan, T. M., E. McWhinnie, B. Driscoll, and R. J. Watson.** 1991. Complex symbiotic phenotypes result from gluconeogenic mutations in *Rhizobium meliloti*. Mol. Plant Microbe Interact. **4:**386–392.
8. **Finan, T. M., J. M. Wood, and D. C. Jordan.** 1983. Symbiotic properties of C_4-dicarboxylic acid transport mutants of *Rhizobium leguminosarum*. J. Bacteriol. **154:**1403–1413.
9. **Grzemski, W., J. P. Akowski, and M. L. Kahn.** 2005. Probing the *Sinorhizobium meliloti*-alfalfa symbiosis using temperature-sensitive and impaired-function citrate synthase mutants. Mol. Plant Microbe Interact. **18:**134–141.
10. **Johnston, A. W. B., and J. E. Beringer.** 1975. Identification of the *Rhizobium* strains in pea root nodules using genetic markers. J. Gen. Microbiol. **87:**343–350.
11. **Karunakaran, R., V. K. Ramachandran, J. C. Seaman, A. K. East, B. Moushine, T. H. Mauchline, J. Prell, A. Skeffington, and P. S. Poole.** 2009. Transcriptomic analysis of *Rhizobium leguminosarum* biovar viciae in symbiosis with host plants *Pisum sativum* and *Vicia cracca*. J. Bacteriol. **191:**4002–4014.
12. **Krishnan, H. B., W. S. Kim, J. Sun-Hyung, K. Y. Kim, and G. Q. Jiang.** 2003. Citrate synthase mutants of *Sinorhizobium fredii* USDA257 form ineffective nodules with aberrant ultrastructure. Appl. Environ. Microbiol. **69:**3561–3568.
13. **Lodwig, E. M., A. H. F. Hosie, A. Bourdes, K. Findlay, D. Allaway, R. Karunakaran, J. A. Downie, and P. S. Poole.** 2003. Amino-acid cycling drives nitrogen fixation in the legume-*Rhizobium* symbiosis. Nature **422:**722–726.
14. **McDermott, T. R., and M. L. Kahn.** 1992. Cloning and mutagenesis of the *Rhizobium meliloti* isocitrate dehydrogenase gene. J. Bacteriol. **174:**4790–4797.
15. **McKay, I., A. Glenn, and M. J. Dilworth.** 1985. Gluconeogenesis in *Rhizobium leguminosarum* MNF3841. J. Gen. Microbiol. **131:**2067–2073.
16. **McKay, I. A., M. J. Dilworth, and A. R. Glenn.** 1989. Carbon catabolism in continuous cultures and bacteroids of *Rhizobium leguminosarum* MNF3841. Arch. Microbiol. **152:**606–610.
17. **Mitsch, M. J., A. Cowie, and T. M. Finan.** 2007. Malic enzyme cofactor and domain requirements for symbiotic N_2 fixation by *Sinorhizobium meliloti*. J. Bacteriol. **189:**160–168.
18. **Mitsch, M. J., R. T. Voegele, A. Cowie, M. Osteras, and T. M. Finan.** 1998. Chimeric structure of the $NAD(P)^+$- and $NADP^+$-dependent malic enzymes of *Rhizobium* (*Sinorhizobium*) *meliloti*. J. Biol. Chem. **273:**9330–9336.
19. **Mortimer, M. W., T. R. McDermott, G. M. York, G. C. Walker, and M. L. Kahn.** 1999. Citrate synthase mutants of *Sinorhizobium meliloti* are ineffective and have altered cell surface polysaccharides. J. Bacteriol. **181:**7608–7613.
20. **Newton, W. E.** 2000. Nitrogen fixation in perspective, p. 3–8. *In* F. O. Pedrosa, M. Hungria, M. G. Yates, and W. E. Newton (ed.), Nitrogen fixation: from molecules to crop productivity. Kluwer, Dordrecht, Netherlands.
21. **Oldroyd, G. E. D., and J. A. Downie.** 2008. Coordinating nodule morphogenesis with rhizobial infection in legumes. Annu. Rev. Plant Biol. **59:**519–546.
22. **Poole, P. S., N. A. Schofield, C. J. Reid, E. M. Drew, and D. L. Walshaw.** 1994. Identification of chromosomal genes located downstream of *dctD* that affect the requirement for calcium and the lipopolysaccharide layer of *Rhizobium leguminosarum*. Microbiology **140:**2797–2809.
23. **Prell, J., B. Boesten, P. Poole, and U. B. Priefer.** 2002. The *Rhizobium leguminosarum* bv. *viciae* VF39 γ-aminobutyrate (GABA) aminotransferase gene (*gabT*) is induced by GABA and highly expressed in bacteroids. Microbiology **148:**615–623.
24. **Prell, J., and P. Poole.** 2006. Metabolic changes of rhizobia in legume nodules. Trends Microbiol. **14:**161–168.
25. **Prell, J., J. P. White, A. Bourdes, S. Bunnewell, R. J. Bongaerts, and P. S. Poole.** 2009. Legumes regulate Rhizobium bacteroid development and persistence by the supply of branched-chain amino acids. Proc. Natl. Acad. Sci. U. S. A. **106:**12477–12482.
26. **Prentki, P., and H. M. Krisch.** 1984. *In vitro* insertional mutagenesis with a selectable DNA fragment. Gene **29:**303–313.
27. **Quandt, J., and M. F. Hynes.** 1993. Versatile suicide vectors which allow direct selection for gene replacement in Gram-negative bacteria. Gene **127:**15–21.
28. **Reid, C. J., and P. S. Poole.** 1998. Roles of DctA and DctB in signal detection by the dicarboxylic acid transport system of *Rhizobium leguminosarum*. J. Bacteriol. **180:**2660–2669.
29. **Ronson, C. W., P. Lyttleton, and J. G. Robertson.** 1981. C_4-Dicarboxylate transport mutants of *Rhizobium trifolii* form ineffective nodules on *Trifolium repens*. Proc. Natl. Acad. Sci. U. S. A. **78:**4284–4288.
30. **Rosendahl, L., C. P. Vance, and W. B. Pedersen.** 1990. Products of dark CO_2 fixation in pea root nodules support bacteroid metabolism. Plant Physiol. **93:**12–19.
31. **Salminen, S. O., and J. G. Streeter.** 1992. Labeling of carbon pools in *Bradyrhizobium japonicum* and *Rhizobium leguminosarum* bv *viciae* bacteroids following incubation of intact nodules with $^{14}CO_2$. Plant Physiol. **100:**597–604.
32. **Sambrook, J., and D. W. Russell.** 2001. Molecular cloning: a laboratory manual, 3rd ed. Cold Spring Harbor Laboratory Press, Cold Spring Harbor, NY.
33. **Schafer, A., A. Tauch, W. Jager, J. Kalinowski, G. Thierbach, and A. Puhler.** 1994. Small mobilizable multipurpose cloning vectors derived from the *Escherichia coli* plasmids pK18 and pK19: selection of defined deletions in the chromosome of *Corynebacterium glutamicum*. Gene **145:**69–73.
34. **Shah, R., and D. W. Emerich.** 2006. Isocitrate dehydrogenase of *Bradyrhizobium japonicum* is not required for symbiotic nitrogen fixation with soybean. J. Bacteriol. **188:**7600–7608.

35. **Thony-Meyer, L., and P. Kunzler.** 1996. The *Bradyrhizobium japonicum* aconitase gene (*acnA*) is important for free-living growth but not for an effective root-nodule symbiosis. J. Bacteriol. **178:**6166–6172.
36. **Walshaw, D. L., A. Wilkinson, M. Mundy, M. Smith, and P. S. Poole.** 1997. Regulation of the TCA cycle and the general amino acid permease by overflow metabolism in *Rhizobium leguminosarum*. Microbiology **143:**2209–2221.
37. **White, J., J. Prell, E. K. James, and P. Poole.** 2007. Nutrient sharing between symbionts. Plant Physiol. **144:**604–614.
38. **Yarosh, O. K., T. C. Charles, and T. M. Finan.** 1989. Analysis of C_4-dicarboxylate transport genes in *Rhizobium meliloti*. Mol. Microbiol. **3:**813–823.
39. **Yurgel, S. N., and M. L. Kahn.** 2004. Dicarboxylate transport by rhizobia. FEMS Microbiol. Rev. **28:**489–501.